SHORT X AND GAMMA BURSTS PRODUCTION BY SWEPT LASER BUNCH

A. Mikhailichenko
Cornell University, LEPP, Wilson Laboratory, Ithaca, NY 14853

We described here the way of production of ≤ 100 fs bursts of X and gamma radiation by Compton back-scattering of a laser bunch which have been swept along the electron trajectory. In the method described the time duration of the secondary radiation does not depend on electron bunch length and is shorter than duration of the primary laser bunch by factor $1/N_R$ –the number of resolved spots of sweeping device (~1/100). The method of the laser bunch sweeping is also helpful in obtaining short electron bunches from a photo cathode.

INTRODUCTION

An idea on generation of X-rays and gammas by Compton back-scattering was developed many years ago [1,2] and used well in a framework of gamma-gamma collider activity [3]. This idea was applied to a circular machine also [4,5]. In this method accommodated to a circular machine the short laser bunch interacts with a passing electron bunch with 90^o across the laser's ray trajectory. In this case the time duration of the secondary radiation defined by the time duty of primary laser radiation $\tau \cong \sigma_b / c$, or by the length of the laser bunch σ_b, or by the length of the electron bunch. In any case the method requires either short primary laser bunch and/or short electron bunch in some modification of the method.

In contrast to this method mentioned above, in our publication [6] we described so called laser undulator installed in Tabletop accelerator. This accelerator developed as a side product in a framework of high-energy linear collider [7-9]. Main difference of our proposal from others is that here we used ***swept*** laser bunch, having slope of 45 degree to direction of propagation in the region of interaction between laser and electron bunches. The laser bunch of this shape can be generated by appropriately designed sweeping device used in [7-9] for high-energy accelerator.

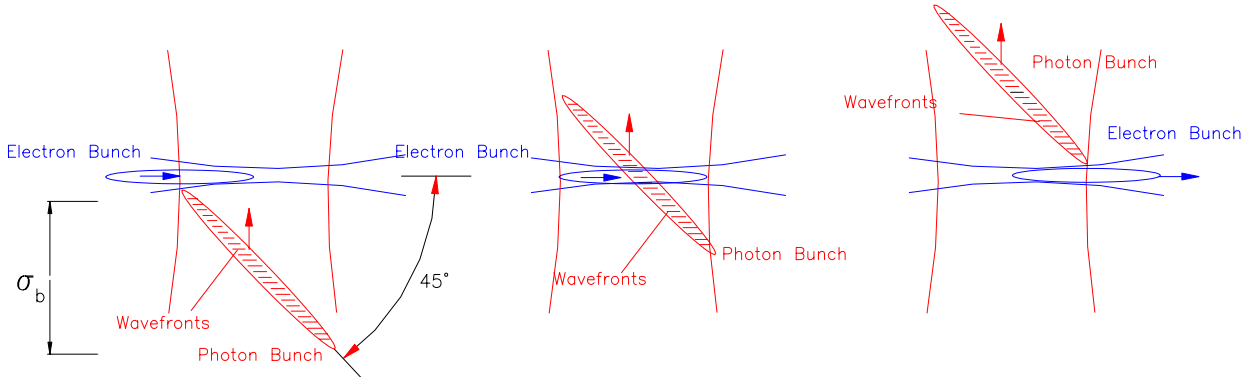

FIGURE 1: Three different times sequences increasing from left to the right. Laser bunch slope with respect to direction of propagation is 45 degrees. Volume with electrons that radiate does not depend on the electron bunch length at all.

In our method the time duration of the secondary radiation is defined by instant ***transverce*** size of the primary laser bunch at location of electron beam trajectory, Fig.1. Meanwhile the total number of radiated secondary particles defined by full length of the laser bunch. With implementation to any damping ring X and gamma ray production with the time duty of the

order of 100 fs or even better can be obtained now with routinely operational laser having bunch of ~30 ps.
Here we describe this method in more detail. We are not describing here the way of generation the laser bunches with duration ~ 30 ps as primary ones due to its' routine nature. It needs to be mentioned however that the repetition rate of a sequence of laser bunches must be synchronized with the bunch pattern in a damping ring (even on stroboscopic basis).

SCHEME

The arrangements of the scene are represented in Fig. 2 as a plan and isometric views.

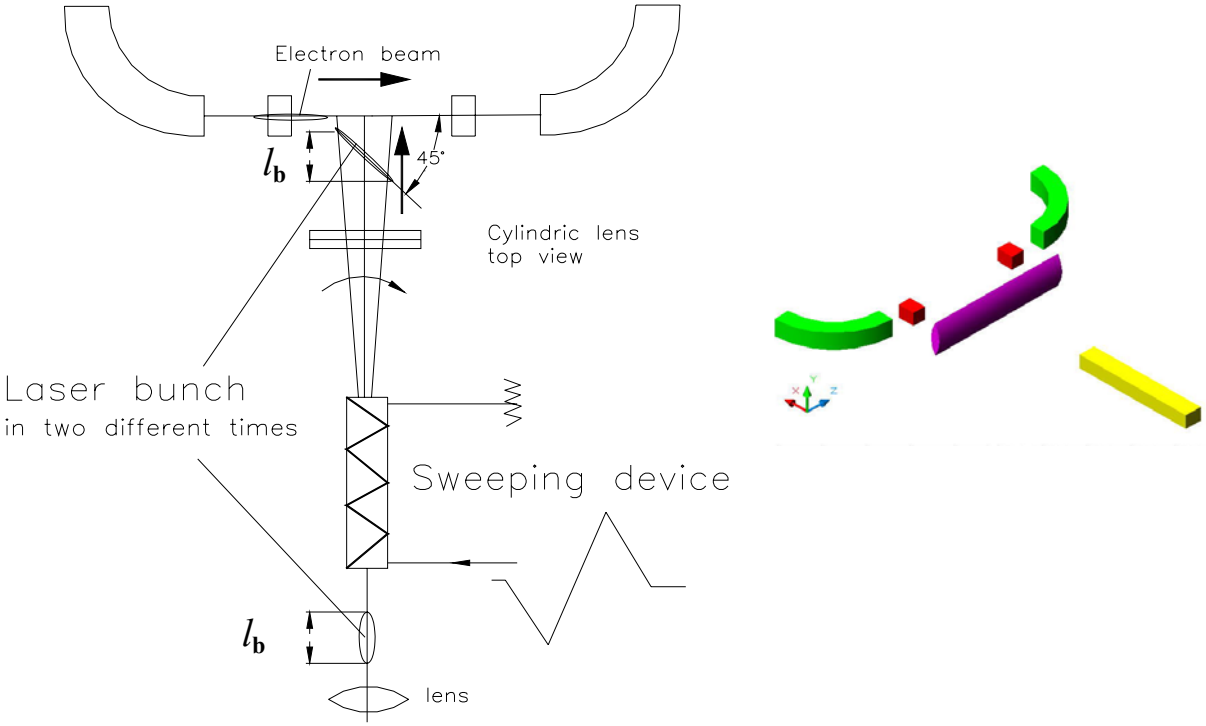

FIGURE 2: Sweeping device deflects the front of laser bunch to the left on the picture plan, the tail of the laser bunch is deflected to the right of the plan. Isometric view for better indication orientation of cylindrical lens is represented at the right. Lens at the lower edge of the figure focuses the primary laser bunch onto the interaction region.

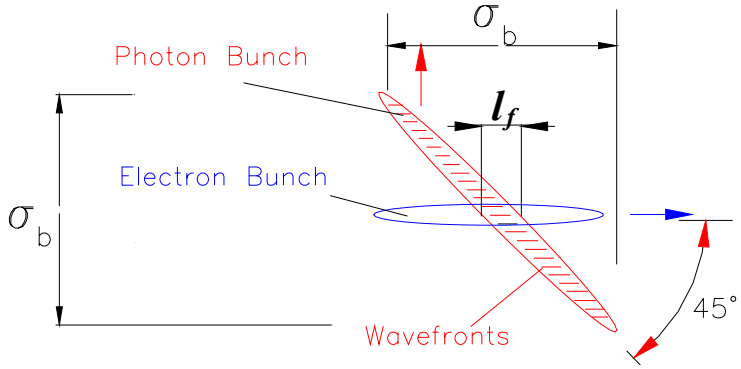

FIGURE 3: Scaled view of central part from Fg.1. Despite the primary laser bunch has the length σ_b, the length of interaction (radiation) region is l_f which defined by the number of resolved spots of sweeping device (see lower).

One can see that the number of electrons effectively interacting with the photon bunch is lower than the bunch population in factor l_f / σ_b, namely this moving length l_f describes radiating electrons.

As far as cylindrical lens, in can be mentioned that it is working with broadband radiation, so the dispersion may play some role in widening the pulse. Utilization of optical materials with appropriate frequency bandwidth is not a problem however.

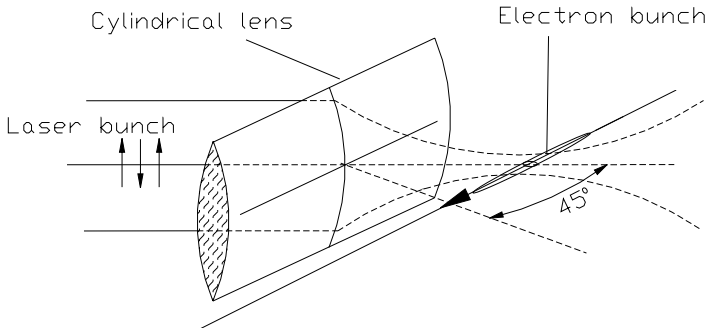

FIGURE 4: Cylindrical lens shrinks the transverse size of the laser bunch in vertical direction. Low dispersion material of the lens allows proper focusing of short bunch.

Circular or elliptical polarization could be obtained also if the primary laser beam has circular or elliptical polarization.

YILD OF SECONDARY PHOTONS

The photon generation in laser undulator could be treated as Compton back-scattering. The rate of the secondary photons generation defined by *K* factor, $K = eH\lambda_u / 2\pi mc^2$, where λ_u –is the undulator period, *H*–is magnetic field value. In our case λ_u is the wavelength of the primary laser radiation. As the radiation is orthogonal to the beam's trajectory, the maximal frequency is the same as defined for ordinary undulator. The quantum effects become significant when energy of the secondary quanta becomes comparable with the particle's energy.

First of all, for the undulator radiation the number of photons, radiated at first harmonic by every particle, could be written as the following

$$N_\gamma \cong 4\pi\alpha \frac{\sigma_b}{\lambda_u} \frac{K^2}{1+K^2} \cong 4\pi\alpha \frac{\sigma_b}{\lambda_u} \frac{e^2 H^2 \lambda_u^2}{4\pi^2 m^2 c^4} \approx \sigma_b \, r_0^2 \frac{H^2}{\hbar\omega}, \qquad (1)$$

where σ_b is the length of undulator, i.e. length of swept primary radiation, see Fig.3, $\omega = c / \lambda_u$, and we substitute here the *K* value.

The term $\frac{H^2}{\hbar\omega}$ can be treated as the photon density, $n_\gamma \cong \frac{H^2}{\hbar\omega}$. So the formula (1) can be rewritten as $N_\gamma \cong \sigma_b \sigma_\gamma n_\gamma$, where $\sigma_\gamma \cong r_0^2$ is Thomson cross section of photon-electron scattering. This introduces the length of interaction as usual $l_\gamma \cong 1/\sigma_\gamma n_\gamma$, so the number of photons per initial particle is simply $N_\gamma \cong \sigma_l / l_\gamma$.

Let $\hbar\omega_0$, $\hbar\vec{k}_0$ be the energy and momentum of incoming photon, $\hbar\omega'$, $\hbar\vec{k}'$ –the energy and momentum of the backward scattered gamma-quanta. Then these parameters linked by the Compton formula [10]

$$\omega_0(1-\frac{v}{c}Cos\vartheta)-\omega'(1-\frac{v}{c}Cos\vartheta')=\frac{\hbar\omega_0\omega'}{mc^2\gamma}(1-\frac{v}{c}Cos\hat{\vartheta}) \quad , \tag{2}$$

where $v=|\vec{v}|$ and $mc^2\gamma$ are initial velocity and the energy of incoming electron, ϑ and ϑ' are the angles between $\vec{v}$ and wave vectors $\vec{k}_0$ and $\vec{k}'$ respectively, $\hat{\vartheta}$ is the angle between $\vec{k}_0$ and $\vec{k}'$, see Fig. 5.

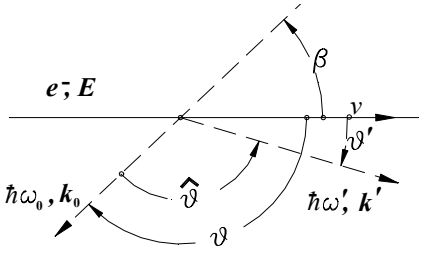

FIGURE 5: Kinematics of the Compton scattering.

Introducing the angle β between the line of incoming photon and the vector $\vec{v}$ as it is shown on the Fig. 5, and supposing that $\vartheta' \approx 1/\gamma$, one can obtain the energy of the backward scattered photon [3,10]

$$\hbar\omega'=\frac{mc^2\gamma\cdot X\cdot Cos^2(\beta/2)}{1+\gamma^2\vartheta'^2+XCos^2(\beta/2)}=\frac{\hbar\omega'_{\max}}{1+\dfrac{\gamma^2\vartheta'^2}{1+X\cdot Cos^2(\beta/2)}} \quad , \tag{3}$$

where

$$X=\frac{4\gamma^2\hbar\omega_0}{mc^2\gamma}=\frac{4\gamma\hbar\omega_0}{mc^2} . \tag{4}$$

So the formula (3) for the secondary photon energy becomes

$$\hbar\omega'_{\max}=\frac{4\gamma^2\hbar\omega_0\cdot Cos^2(\beta/2)}{1+X\cdot Cos^2(\beta/2)}=mc^2\gamma\frac{x}{1+x} , \tag{5}$$

$x=X\cdot Cos^2(\beta/2)$. One can see, that dimensionless parameter X is proportional to the ratio of the photon energy in the electron rest frame to the electron's rest energy.
In the case of wiggler $\beta=\pi/2$, and $x=X/2$ and formula (3) becomes

$$\hbar\omega'=\frac{mc^2\gamma\cdot X/2}{1+\gamma^2\vartheta'^2+X/2}=\frac{\hbar\omega'_{\max}}{1+\dfrac{2\gamma^2\vartheta'^2}{1+X}} \tag{6}$$

For a primary laser radiation with a wavelength around micrometer, $\hbar\omega_0 \cong 1eV$, x parameters and energy of secondary photons are represented in Table 1.

TABLE 1

E, GeV	*x*	$\hbar\omega'$, *MeV*
0.1	0.00077	0.077
1.0	0.0077	0.77
10.	0.077	711
100.	0.77	43370

All secondary photons are moving in the same sample having the longitudinal length of l_f in Fig.3. Namely this distance defines the duty time for secondary radiation.

Let us estimate the photon flux. For a micrometer level of the primary wavelength the number of resolved spots $N_R \sim 100$ can be expected. So the longitudinal size of the laser spot on the line along the electron's trajectory for $30ps$ primary laser bunch will be $l_f \cong \sigma_b / N_R \cong 1cm/100 \sim 100\mu m$. Vertical size of the laser radiation defined by cylindrical lens and can be estimated as ~5 μm. So the effective volume of interaction for single particle with this $30ps$-laser flash could be estimated as $V \cong 1cm \times 100\mu m \times 5\mu m \cong 5 \cdot 10^{-6} cm^3$. Here we suggested that the waist of the laser radiation be in synchronism with electron bunch. The number of primary photons can be calculated as

$$N_{0\gamma} \cong E_{flash} / \hbar\omega_0 . \tag{7}$$

The photon density and the length of interaction go respectively

$$n_\gamma \cong N_\gamma / V , \qquad l_{eff}^{-1} \cong n_\gamma \sigma_T = n_\gamma \tfrac{8\pi}{3} r_0^2 . \tag{8}$$

Total number of secondary photons goes to

$$N_\gamma \cong N_{eff} \frac{\sigma_b}{l_{eff}} , \tag{9}$$

where $N_{eff} \cong N \cdot l_f / \sigma_b \cong N / N_R$ is effective number of electrons interacting with primary laser bunch, N_R is the number of resolved spots described lower, N is the bunch population. For the laser flash with, say $E_{flash} \cong 1mJ$, $\hbar\omega_0 \cong 1eV$, the number of primary photons goes to $N_{0\gamma} \cong 6.25 \times 10^{15}$. So the photon density goes to $n_\gamma \cong N_{0\gamma} / V \cong 1.25 \cdot 10^{21}\ cm^{-3}$ and length of interaction goes to $l_{eff}^{-1} \cong n_\gamma \sigma_T = n_\gamma \tfrac{8\pi}{3} r_0^2 \cong 1.25 \cdot 10^{21} [\tfrac{1}{cm^3}] \cdot 6.65 \cdot 10^{-25} [cm^2] = 8.3 \cdot 10^{-4} cm^{-1}$, so $l_{eff} \cong 12.5m$. The last means that each electron radiates in average $N_\gamma \cong \sigma_l / l_\gamma \cong 8.3 \cdot 10^{-4}$ photons per pass.

For $N \cong 10^{10}$ this brings the photon number to $N_\gamma \cong 8.3 \cdot 10^4 / bunch / pass$. Suggesting repetition rate $100kHz$ one can expect the photon flux $\dot{N}_\gamma \cong 8.3 \cdot 10^7 s^{-1}$. Total power from laser goes to $10mJ \times 10^5 \tfrac{1}{s} = 100W$. These numbers gave an idea of the possibilities of the method proposed.

The brightness of the source can be evaluated as the following

$$B \cong \frac{\dot{N}_\gamma}{(\gamma\varepsilon) \cdot (\beta/\gamma)\gamma^{-2}} = \frac{\gamma^3 \cdot \dot{N}_\gamma}{(\gamma\varepsilon) \cdot \beta} \tag{10}$$

If we suggest that the electron beam emittance be $\gamma\varepsilon \cong 3 \cdot 10^{-3} cm \cdot rad$, envelope function in the region of interaction as $\beta \cong 1cm$, then one can estimate for $\gamma \cong 10^4$

$$B \cong 8.3 \cdot 10^{24}\ photons / cm^2 / rad^2 / \sec .$$

Let us remind that the duty time for these bursts of radiation is about 100 fs, despite the primary length of laser bunch is ~30ps. Some optimization is possible in direction of shortening the primary bunch. Then as the number of resolved spots remains the same, the length of interaction region can be shortened adequately.

Formula for effective length of interaction (8) written with Thomson's cross-section. It is not difficult however to take cross section which takes into account relativistic effects [10].
Dependence is weak however. $\sigma_C \cong \frac{8\pi}{3} r_0^2 (1-x),\ x<<1$, $\sigma_C \cong \frac{2\pi}{x} r_0^2 (\log x + \frac{1}{2}),\ x>>1$.

SWEEPING DEVICE

The devices types suitable for the sweeping were collected in [8] (see references there; below we represent some materials from this publication). Each sweeping device uses controllable deflection of the laser radiation in time.
Any deflecting device could be characterized by a deflection angle ϑ and the angle of natural diffraction $\vartheta_d \cong \lambda / a$, where *a* —is the aperture of the sweeping device, λ is a wavelength. The ratio of deflection angle to diffraction angle is a fundamental measure of quality for any deflecting device. This ratio defines the *number of resolved spots (pixels)* along the sweeping line, $N_R = \vartheta / \vartheta_d$. Also the deflection angle could be increased by appropriate optics, the number of resolved spots N_R is *an invariant* under such transformations. As one can see, N_R value gives the number for the duty time reduction.
Electro-optical sweeping device uses controllable dependence of refractive index on electrical field strength and direction applied to some crystals. With abbreviation $\Delta(1/n)_i = 1/n_i - 1/n_{0i}$ the refractive index dependence in active media could be written as the following

$$1/n_i^2 = 1/n_{0i}^2 + \sum_j r_{ij} \cdot E^j ,$$

or in more detail

$$\begin{pmatrix} \Delta(1/n^2)_1 \\ \Delta(1/n^2)_2 \\ \Delta(1/n^2)_3 \\ \Delta(1/n^2)_4 \\ \Delta(1/n^2)_5 \\ \Delta(1/n^2)_6 \end{pmatrix} = \begin{pmatrix} r_{11} & r_{12} & r_{13} \\ r_{21} & r_{22} & r_{23} \\ r_{31} & r_{32} & r_{33} \\ r_{41} & r_{42} & r_{43} \\ r_{51} & r_{52} & r_{53} \\ r_{61} & r_{62} & r_{63} \end{pmatrix} \times \begin{pmatrix} E_x \\ E_y \\ E_s \end{pmatrix}, \qquad (11)$$

where the vector $\vec{E} = \{E_x, E_y, E_s\}$ describes the electrical driving field applied, where r_{ij}–are 6×3 tensor. Index *i* runs from 1 to 6. 1 stands for *xx*, 2–for *yy*, 3– *ss*, 4– for *ys*, 5–for *xs*, 6– for *xy*, *s*-longitudinal coordinate. Indicatrix allows to determinate the refraction index *n* components for monochromatic plane waves as a function of their polarization.
The change of reflecting index is equal to $\Delta n_i \cong (\partial n_i / \partial E_j) E^j(t)$. The (11) yields $\partial n_i / \partial E_j = -n_{0i}^3 r_{ij} / 2$ and the net change of refractive index becomes

$$\Delta n_i \cong (\partial n_i / \partial E_j) E^j(t) \cong -n_{0j}^3 r_{ij} E^j / 2 \qquad (12)$$

For the parameters under discussion at the deflecting device, the power density of the laser radiation is much smaller than this driving external field.
Typical values of the r_{ij} are of the order $\cong 10^{-12} m/V$. For example, for *GaAs (ZnSe, CdTe)* cubic structure and for *KDP (ADP, CdGeAs2)* tetragonal structure we have respectively

$$(r)_{ij} = \begin{pmatrix} 0 & 0 & 0 \\ 0 & 0 & 0 \\ 0 & 0 & 0 \\ 1.5 & 0 & 0 \\ 0 & 1.5 & 0 \\ 0 & 0 & 1.5 \end{pmatrix} \times 10^{-12}[m/V], \qquad (r)_{ij} = \begin{pmatrix} 0 & 0 & 0 \\ 0 & 0 & 0 \\ 0 & 0 & 0 \\ 8.8 & 0 & 0 \\ 0 & 8.8 & 0 \\ 0 & 0 & 10.5 \end{pmatrix} \times 10^{-12}[m/V] \qquad (13)$$

So the cut must be made so that the prisms have their orthogonal edges parallel to principal axes. For a prism-based device, Fig.6, deflecting angle is defined by the phase delay across the laser beam front arising from differences in the path lengths in material of the prism having a refractive index *n*.

$$\vartheta \cong n\frac{(L_a - L_b)}{w}. \qquad (14)$$

Here *w* –is the width of incident laser beam, L_a and L_b –are the distances through which the edges of the laser beam traverse the prism, Fig.6. A change in refractive index value yields a deflection angle change. To arrange such a change in refraction index, the basements of the prism are covered by metallization. When a voltage *V*(*t*) applied to the metallization, the refractive index changes $\Delta n = \Delta n(V(t))$, what yields the change in deflection angle as

$$\Delta\vartheta \cong \Delta n\frac{(L_a - L_b)}{w}. \qquad (15)$$

For such a sweeping device, a lot of electro-optical crystals can be used, see Table 2 below. For example, a crystal *KDP* (KH_2PO_4) is transparent for a radiation with the wavelength $\lambda \cong 0.2 \div 1\,\mu m$. Some other crystals, such as a *CdTe*, *CuCl, GaAs*, *ZnTe, ZnS* are transparent in the region of wavelengths around $\lambda \approx 10\,\mu m$. The last group of materials have rather high refractive indexes n_0~(2-4) what compensate smaller electro- optical coefficient.

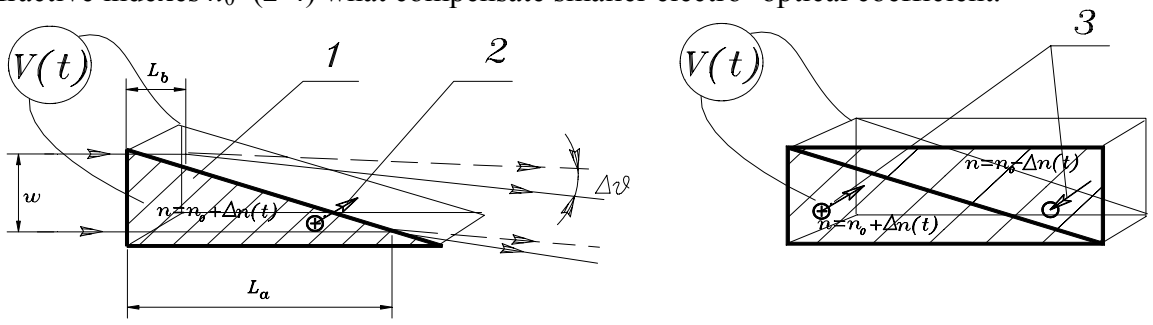

FIGURE 6: The prism deflection device concept. At the left side, the electro-optical crystal prism has metallization 1 (hatched) on both basements of the prism. 2 shows direction of optical axis. Time dependent voltage applied to metallization. At the right side *two* prisms have oppositely oriented optical axes 3 with the same polarity of electrical field applied.

The number of resolvable sports N_R for this device can be found as

$$N_R \cong \frac{\Delta\vartheta}{\lambda/a} = \frac{\Delta n \cdot (L_a - L_b)\cdot a}{\lambda \cdot w} \cong \Delta n\frac{l}{\lambda}, \qquad (16)$$

where $l = L_a - L_b$ stands for the prism base length and $a / w = 1$ in our case (a is geometrical aperture). Substitute for example the numbers for *ZnTe* (transparent for CO_2 laser radiation) which has $n_o \approx 2.9$, $r_{41} \cong 4.4 \cdot 10^{-12} m/V$, $E \cong 10 kV/cm \equiv 10^6 V/m$ one can obtain $\Delta n \cong 10^{-4}$. For *KTN* (*Potassium Tantalate Niobat*) crystal $\Delta n \cong 7 \cdot 10^{-3}$ for $\lambda \cong 0.63 \mu m$ is possible (see references in [8]). Anyway, the shorter wavelength is preferable from this point of view.

One can see from (11) and (12) that with the increase in optic path difference both the deflection angle and the number of resolved spots increase also.
To increase the last numbers (N_R, $\Delta\vartheta$), *multiple-prism* deflectors were developed, see Fig.7. We suggested a *traveling wave* regime here to be able to sweep the short laser bunch [8]. The plates are wider in transverse direction, than the prisms. This has done for uniform field generation in the volume of crystals. Some electrostatic optimization could be done easily.
Here neighboring prismatic crystals have oppositely oriented optical axes. These crystals positioned between the strip–line electrodes. To be able to sweep short laser bunches, the voltage pulse $V(t)$ is propagating along this strip-line as a *traveling wave* together with the laser bunch to be swept, [8]. This gives the necessary voltage profile along the laser pulse at *cm* distances, what corresponds to the pulse duration $c\tau$.

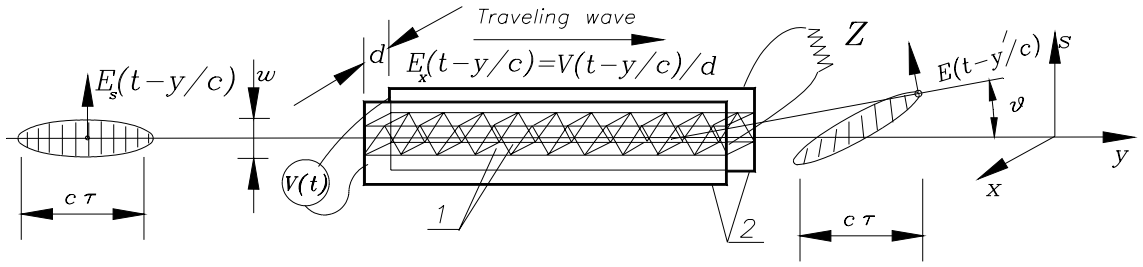

FIGURE 7 [8]: Prisms 1 with *oppositely directed optical axes* installed in series between two parallel strip–line electrodes 2, *d*–is the distance between them. *Z*– is matching impedance. Lines across the laser bunch schematically show the wave fronts. $E_x(t - y/c)$–is a driving electrical field.

As we mentioned, the radiuses of curvature of wavefronts in the swept beam have a common center in the deflecting device. Necessary correction of this effect can be easily done by variation of the thickness of cylindrical lens in Fig.2 for example.
The deflection angle and the number of resolved spots become now

$$|\Delta\vartheta| \cong \Delta n \frac{2L_d}{w} \cong \frac{L_d}{w \cdot d} n_0^3 \cdot r_{ij} \cdot V, \qquad N_R \cong \Delta n \frac{2L_d}{\lambda} \tag{17}$$

Where L_d stands for full length of deflecting device, *w*–is the laser beam width (along direction of deflection). For *L*=50*cm*, one can expect for $w \cong 1cm$, that deflection angle is $\Delta\vartheta \cong 10^{-2}$ and $N_R \cong 10$ for $\lambda \cong 10\mu m$ and, correspondingly $\Delta\vartheta \cong 10^{-2}$ and $N_R \cong 100$ for $\lambda \cong 1\mu m$.
We estimated the field applied to the crystals as 10 *kV/cm*. This is really a field strength *variation* along the laser bunch. This *variation is traveling together with the laser bunch* along the sweeping device, Fig. 7. This strip-line-sweeping device could be sectioned (sliced) for the voltage reduction. For example, utilization of hundred slices in direction orthogonal to $w \cong 1$ *cm* will reduce the voltage to 0.1 *kV* per slice. If we suggest that electrical impedance of the strip-

line be of the order $Z \cong 100\,\Omega$, the impulse power required to generate this voltage becomes $P \cong 100\ W$ per slice, while average one remains on the level $P_{av} \cong P \cdot f \cdot \tau \cong 1mW$ for repetition rate $f \cong 1kHz$ and $c\tau \cong 10cm$. Special devices with avalanche diodes could be used here.

The thickness of the package is defined by the level of the damage to the material of electro–optical crystal. We considered as example the case when the laser flash energy passing through the single crystal is $1mJ$. In our example we estimated the area cowered by the laser beam as $S \cong w \cdot d$, what is about $1cm^2$. This yields the energy density 1 $mJ/\ cm^2$ only. One can decrease the area at least 10 (up to 100) times. Reduction of orthogonal dimension will further reduce the power required for deflection. Some optimization is possible here.

Example of technical realization of this traveling wave deflector is represented in Fig.8 below. Here, basically, the strip-line electrodes 2 have triangle crystals with opposite optical axes orientation (see Figs.6, 7) in between. A para-phase impulse, applied to one end of strip-line trough connectors 3, propagates to the other end and further connected to the matching impedance. So only half of full voltage is applied trough each connector. Matching dielectric 6 adjusts the speed of deflecting wave to the speed of laser radiation, propagating in crystals.

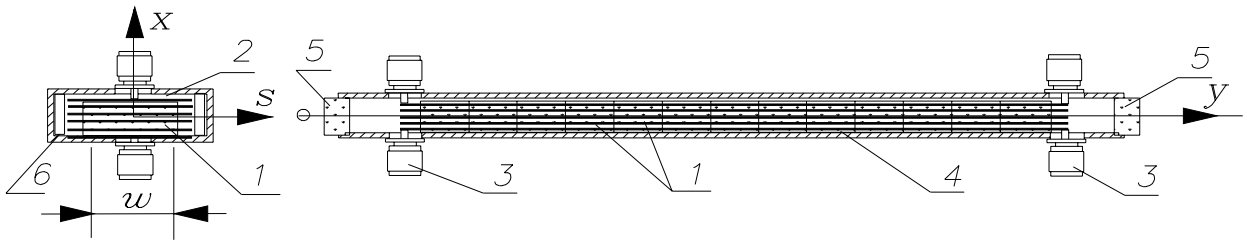

FIGURE 8: Example of technical realization of multi-prism traveling wave sweeping device [8]. Electro-optical crystals 1 are positioned between strip-lines 2, attached at the end to the connectors 3. 4–is a cabinet with optical windows 5 from both sides. 6–is a matching dielectric.

The broad band traveling wave deflector could be obtained also if the same crystals located in the middle of a waveguide shortened from both sides [8].

In Table 2 we summarized general parameters of electro optical deflectors.

TABLE 2

Wavelength	Materials	ϑ, *rad*	N_R
$\lambda \cong 10\mu m$	*GaAs, ZnTe, ZnS, CdS, CdTe, CuCl*	0.01-0.02	10
$\lambda \cong 5\mu m$	*$LiNbO_3$, $LiTaO_3$, CuCl*	0.01-0.02	20
$\lambda \cong 1\mu m$	*KDP, DKDP, ADP, KDA, $LiNbO_3$*	0.01-0.02	100

One can see that shorter wavelengths, especially optical ones, are preferable. For optical wavelengths the same crystals as indicated in lower line of Table 2 could be used successfully. *KTN* (*Potassium Tantalate Niobat*) can be recommended for visible light due to it's ~70 times higher number of resolved spots achievable.

It can be shown (see [8] for details and references) that optimized deflecting device with focusing lens installed in front of it (Fig.2) occupies ~2/3 of the distance between the lens and interaction region.

Mechanical deflection system is also possible here, however this is always a matter of reliability. In case of using quartz it must be taken with cheer cut and must be staged for work as a tandem. Frequency of oscillation of the mirrors can be ~ 5 *MHz* in ten-stage tandem [8].

SHORT BUNCHES FROM A PHOTOCATHODE

The same idea can be applied to the electron bunch production with help of photocathod. Let us consider the scheme represented in Fig. 9 below. Principle of operation is clear however. Laser bunch is swept so that the head is going to the far side of photocathod and the tail is going to the closest side. The speed of sweeping is arranged so that the slope of the laser bunch is parallel to the surface of the photocathod at the moment of touching the laser bunch to the photocathod. The shortage of illumination time increases with increase of illumination angle θ in Fig. 9.

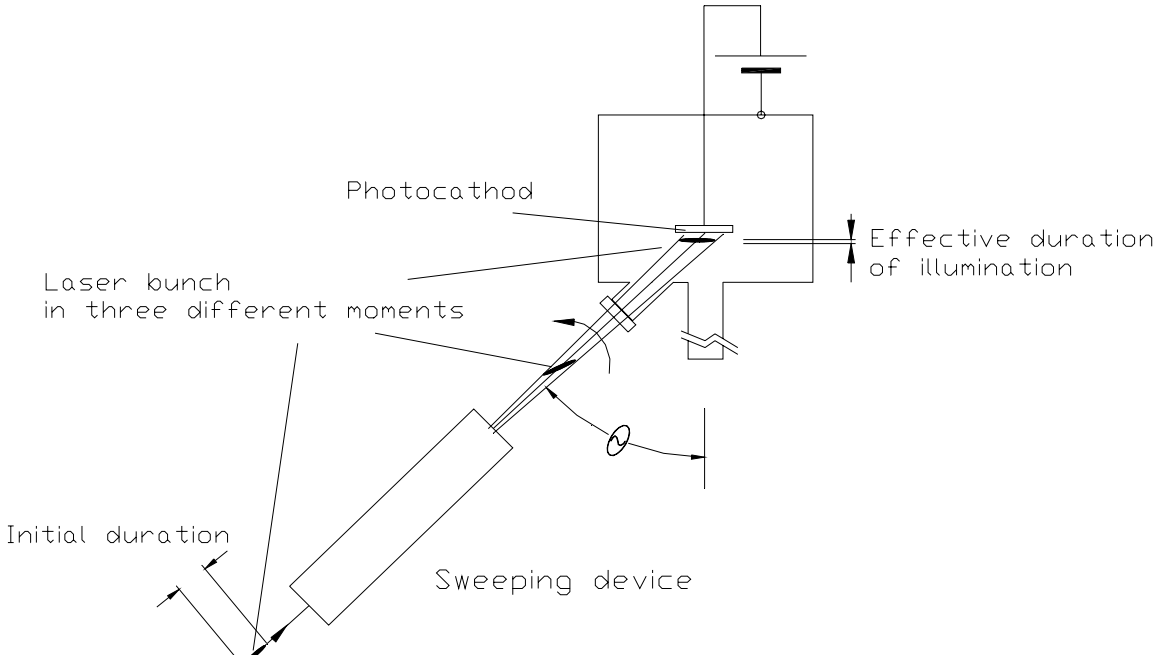

FIGURE 9: Principle of photocathod illumination. The larger angle of illumination θ is –less deflection required. Shortage in illumination time is bigger with increasing of illumination angle θ.

So one can see that practically any existing scheme can be equipped with this sweeping device.

CONCLUSION

The method proposed allows generation of short bunches of secondary photons practically with ordinary equipment. Secondary radiation duty is shorter, than primary laser duty in the number equal to the number of resolved spots for the sweeping device. The last can go to 300 for visible light. Electro-optical sweeping device available on the market and appropriate optics can be easily implemented into the scene. The photon flux of ~30-100 fs of X or gamma radiation is big enough to satisfy the broad variety of user's needs.

The scheme is not sensitive to a jitter of laser or electron beam as the only a small length of electron bunch $l_f \cong \sigma_b / N_R$ radiates and this duration time does not depend on the bunch length at all.

Detailed scheme of laser pattern requires taking into account specifics of damping ring, planned for installation in. Laser with synchronized modes can generate necessary sequence of primary laser bunches.

REFERENCES

[1] F.R. Arutynian, V.A. Tumanian, Phys. Lett., 4(1963), 176.

[2] E.Feinberg, H. Primakoff, *Interaction of Cosmic Ray Primaries with Sunlight and Starlight*, Phys. Rev. 73(1948) 449-469.

[3] I.F.Ginzburg, G.L.Kotkin, V.G.Serbo, V.I.Telnov, NIM 205:47,1983. JETP Lett. 34:491-495, 1981. Pisma Zh. Exp.Teor. Fiz. 34: 514-518, 1981.

[4] K.-J Kim et al., NIMA 341, 351 (1994).

[5] W. Leemans et al., AIP Proc. 1994 Workshop on Advanced Accelerator Concepts, Lake Geneva, LBL –36369.

[6] A. Mikhailichenko, *Table-top accelerator with extremely Bright Beam*, 9th Advanced Accelerator Concept Workshop (AAC2000), Santa Fe, New Mexico, 10-16 Jun., Published in AIP Conf. Proc.569:, 2000. Ibid., pp.-881-889.

[7] A. Mikhailichenko, *Parameters of* 2×200*GeV Linear Collider with Microstructures Excited by Laser Radiation*, ibid., 365-373.

[8] A. Mikhailichenko, *Particle Acceleration in Microstructures Excited by Laser Radiation*, CLNS 00/1662, Cornell 2000, 89 pp.

[9] A. Mikhailichenko, *Particle Acceleration in Microstructures*, SNOWMASS-2001-T401, Jun 2001, 32pp.

[10] V.B. Berestetskii, E.M. Lifshits, L.P. Pitaevskii, *Quantum Electrodynamics*, Pergamon Press, Second Edition, 1982.